Publ. Natl. Astron. Obs. Japan Vol. 6. 65–74 (2001)

Geotechnical Study of ALMA Site Foundation in the Cerro Chascón Science Preserve

Atsushi YASHIMA[1)], Feng ZHANG[1)], Hiroaki SHIGEMATSU[1)], Akihiro ENDO[1)], Kazunori NISHIDA[2)], and Seiichi SAKAMOTO

(Received April 2, 2001)

Abstract

The Nobeyama Radio Observatory of Japan (NRO) is continuing to carry out design and development work on its Atacama Large Millimeter/Submillimeter Array (ALMA) at the area in the Cerro Chascón Science Preserve. In order to construct the larger-scale interferometer with 14 km base line, it is necessary to make a detail survey on the geology, topography and geotechnical properties of the construction site. In this paper, additional to the survey by NRO, such tests as the analysis by X-ray diffractometer, observation by Scanning Electronic Microscope (SEM), pH test, test of resistivity are conducted to understand the geological properties. Furthermore, ultrasonic wave test, uniaxial compression test, slaking test and creep test are conducted to clarify the mechanical behavior in infinitesimal strain condition, the long-term stability and the deterioration of strength of the ground. The results are described in detail.

Key words: ALMA, Geotechnical property, Geological property.

1. Introduction

The project site for ALMA is a fairly flat area at high altitude (approximately 5,000 m above sea level), located at the foot of the Chajnantor and Chascón mountains in the Cerro Chascón Science Preserve, not far from the Jama Pass International Road, about 80 km from the town of San Pedro de Atacama. NRO plans to install an array of large parabolic antennas at the site. The relative positions of the antennas must be determined accurately. Residual delays will result in phase errors which change across the observing band and differential phase errors between two different sources on the sky. Requiring the differential phase error between two sources 5 degrees apart on the sky to be on the order of 5 degrees results in a baseline accuracy of about 0.1 mm. Therefore, frequent baseline calibration should be carried out during antenna operation at the site. The geotechnical characteristics of the foundation have to be also investigated for the design work.

In the present study, firstly the geological features which include mineralogical composition and structure of subsurface pebbles, gravel and rock by the X-ray diffractometer and Scanning Electron Microscope (SEM), pH characteristic and electric resistivity of foundation rock are investigated. Secondly geotechnical characteristics on foundation rock are investigated by a series of laboratory tests. The rigidity is determined by the ultra sonic wave test. The uniaxial compressive strength and long term strength are determined by the conventional uniaxial compression test and multi-stage uniaxial creep test. The potential for disintegration of rock is determined by slaking test.

[1)] Department of Civil Engineering, Gifu University

[2)] OYO Corporation

2. Geological Study on Foundation

The site considered for ALMA project is within the Cerro Chascón Science Preserve and surrounds the Chascón mountain which has an elevation slightly higher than 5,700 m. The area is fairly flat and most of its extension slopes gently to the South. Its mean elevation is about 5,000 m above sea level and it has a number of depressions and other topographic features that make the site uneven. The surface shows a thin layer of gravel and pebbles followed by a few centimeters of sand, although rock outcrops are often observed at the site.

Several stratified units, ranging from Paleozoic to Quaternary, and groups of plutonic rocks, have been distinguished in the overall region. The precordillera and Andean cordillera domain morphostructure contains upper Cenozoic volcanic rocks including the ignimbrite. The Cajon ignimbrite, present at the site, is dated from the Pleistocene-Holocene with 0.8 million years. Its outcrop covers approximately 450 km^2 in the Calama sheet, extending another 530 km^2 to the south. Its thickness ranges from 250 m to a few meters, thinning to the eest.

NRO and NRAO (National Radio Astronomy Observatory) of the United States (2000) summarized the geotechnical study on the subsurface at the proposed site by drilling six borings. The location for the borings is indicated in figure 1. From their report, it is found that the subsurface is characterized by a thin top layer of residual soil (gravel and pebbles) over very broken to broken rock. The depth to massive rock is very shallow ranging from 1.6 to 3.6 m except at Boring No. 5 and 6 sites.

2.1 Mineralogical Composition and Structure of Subsurface

Mineralogical composition of the subsurface including residual soils and massive rock is determined from the

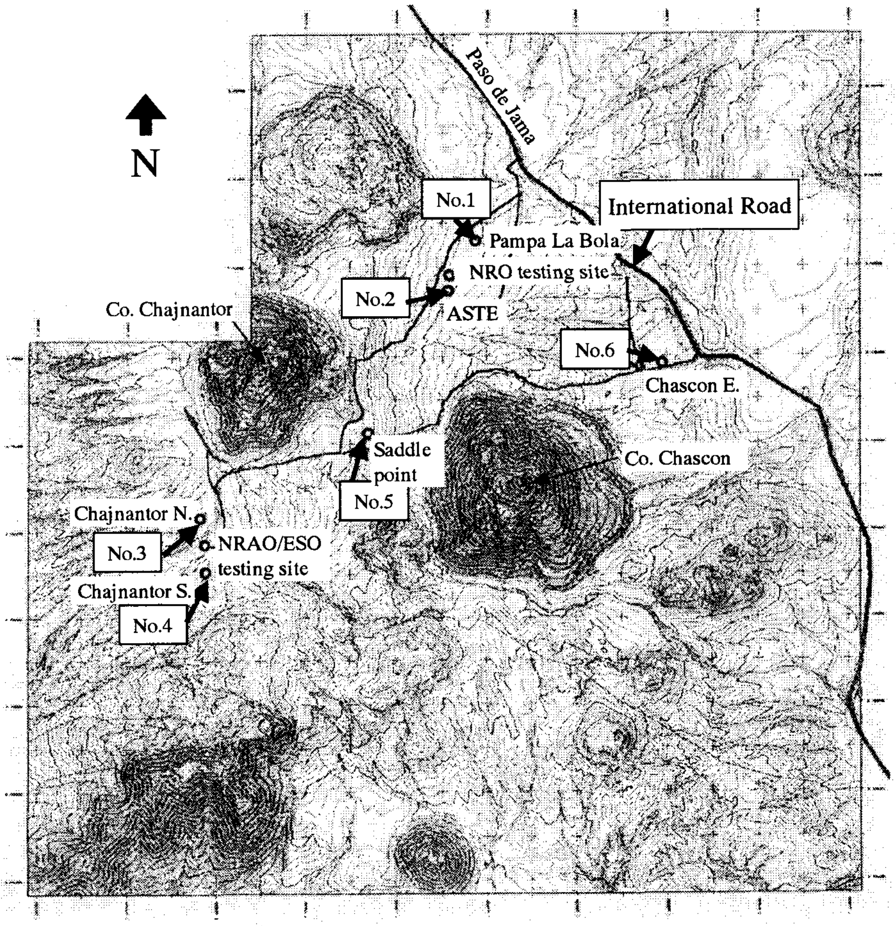

Fig. 1. Location for the borings and international road.

analysis by the X-ray diffractometer. Residual soils sampled at four boring sites and rock outcrop at the Jama Pass International Road are analyzed. The results obtained from different samples are shown together with SEM photographs in figure 2.

The results of the identification are listed in Table 1. From the analysis by X-ray diffractometer, it is found that Feldspar like Sanidine, Orthoclase and Microcline, and Illite are involved in all samples. The mineral that shows a maximum peak value in X-ray diffraction, however, cannot be identified. Therefore, except No. 3 sample, it is unable to conclude that Quartz is not included in the samples. The rock base in this area is made from welded tuff, subjected to the erosion by glacial and weathering. From the borings at all sites, it is found that only several meters at the surface of the rock subjected to light weathering and the rock is rather stable. Except some difference existed in Muscovite, the samples from all these sites are composed of the same minerals.

Figure 2 shows the microstructures of the surface

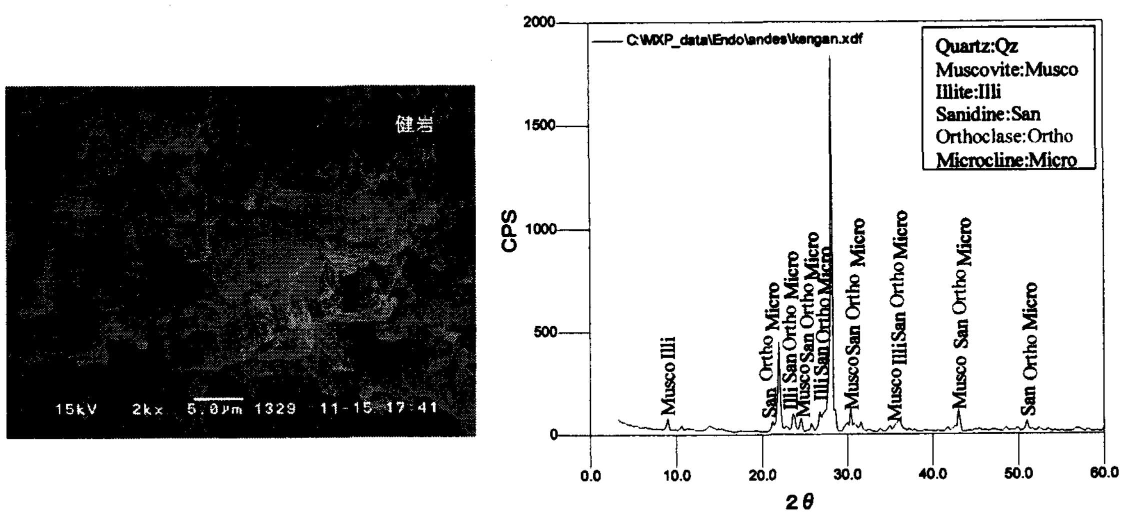

Fig. 2(a). SEM photograph and result by the X-ray diffractometer on intact rock sampled at the international road.

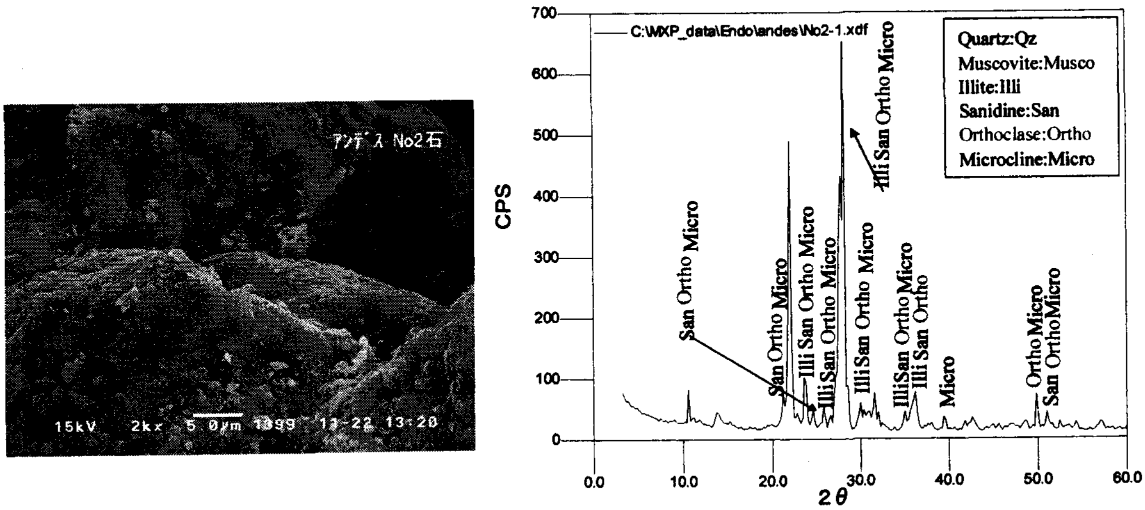

Fig. 2(b). SEM photograph and result by the X-ray diffractometer on pebble samples at No. 2 site.

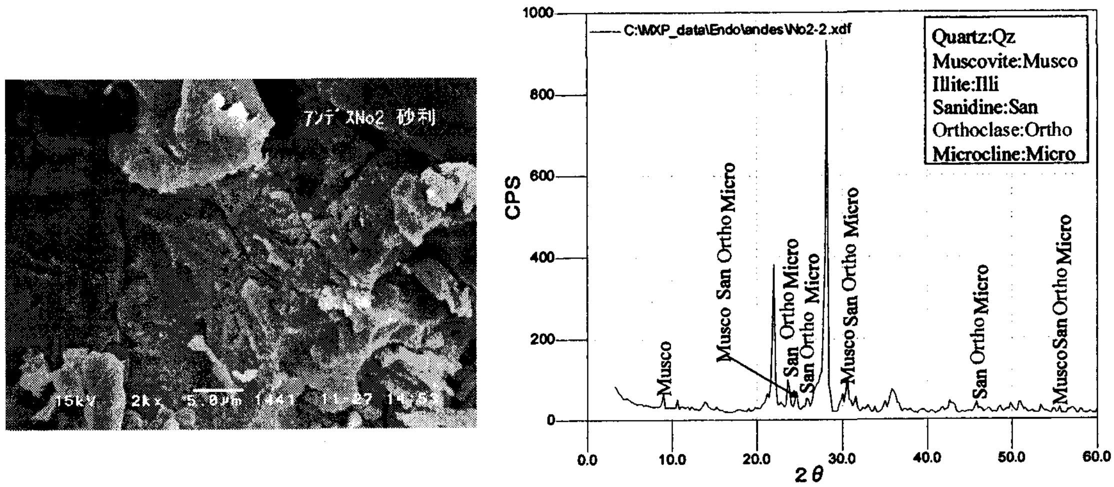

Fig. 2(c). SEM photograph and result by the X-ray diffractometer on sand sampled at No. 2 site.

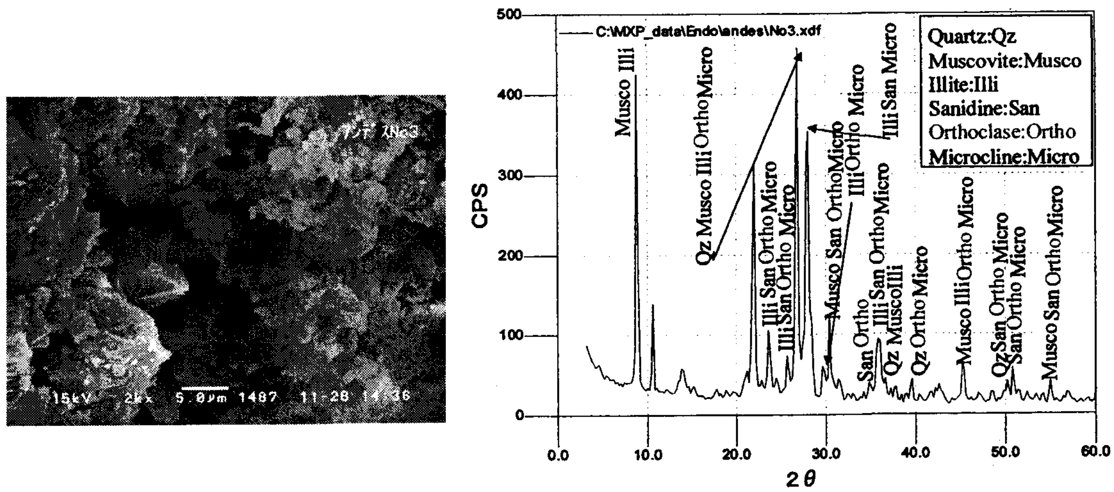

Fig. 2(d). SEM photograph and result by the X-ray diffractometer on pebble sampled at No. 3 site.

layer and the welded tuff from each site. It is known from the figure that the degree of the weathering is different from each other at different sites.

2.2 pH Values

The foundation of the telescopes will be made of concrete according to the design. Therefore, there is a danger that alkali-aggregate reaction takes place because Sanidine that shows alkali is involved in the rock. For this reason, pH test is conducted on the samples from No. 2 site. By using the same sample, uniaxial compression test is also conducted as will be shown in later chapters. The mass of the sample is 545 g and the mass of the water added is 1,432 g. The pH value is measured during 89

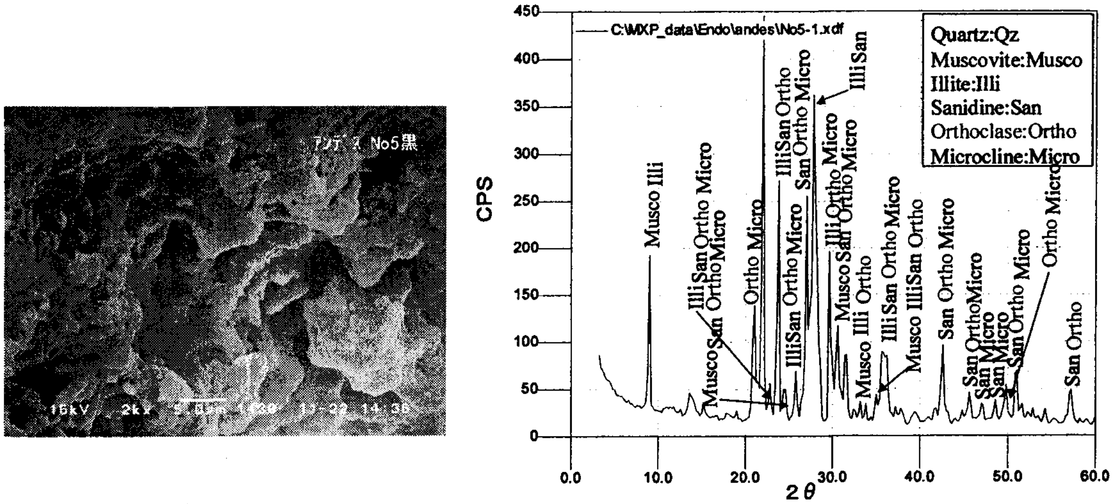

Fig. 2(e). SEM photograph and result by the X-ray diffractometer on black pebble sampled at No. 5 site.

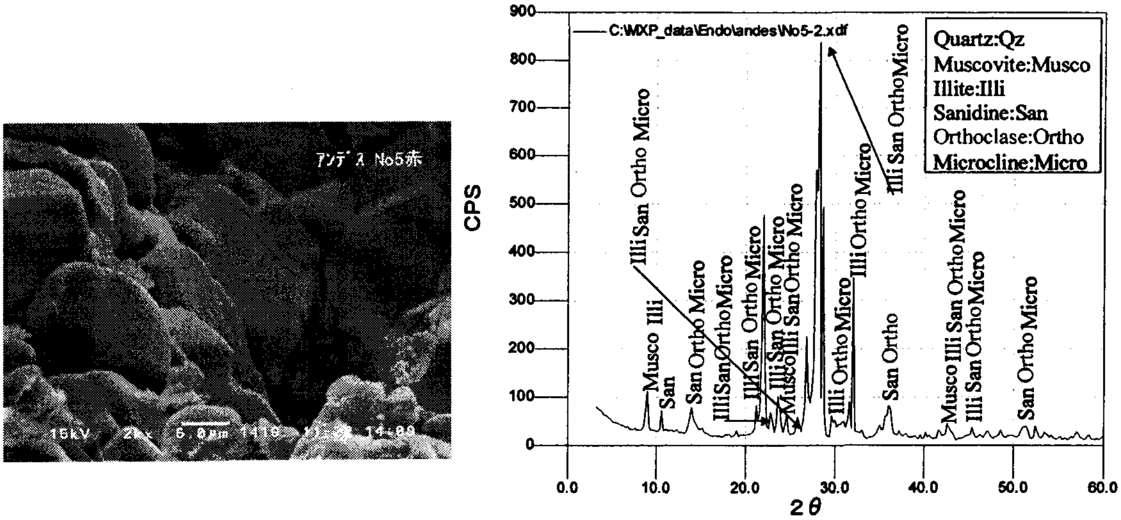

Fig. 2(f). SEM photograph and result by the X-ray diffractometer on red pebble sampled at No. 5 site.

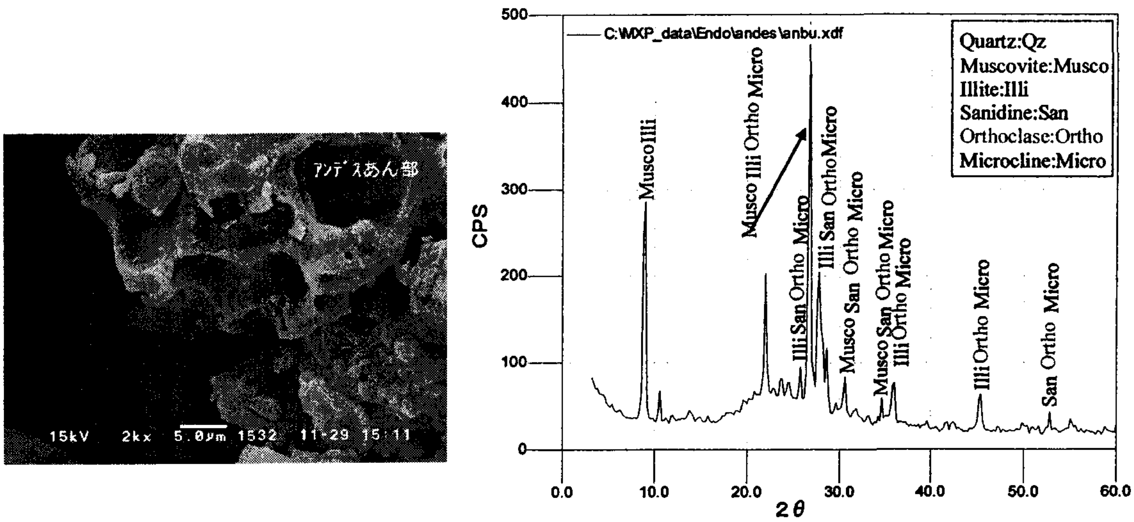

Fig. 2(g). SEM photograph and result by the X-ray diffractometer on sand sampled at No. 5 saddle site.

hours since the sample is immersed into water. The temperature of the tested liquid is 18℃, with a vibration of ±0.3℃. Figure 3 shows the relationship between pH value and the time. From the figure, it is clear that the pH value increases within a very short time. Therefore, more detail discussion on the prevention of the alkali-aggregate reaction in the concrete foundation should be done.

2.3 Resistivities of Soil and Rock

Soil resistivity is a basic parameter necessary for the design of effective grounding and lightning prevention/protection systems. The resistivity of rocks or soil is in

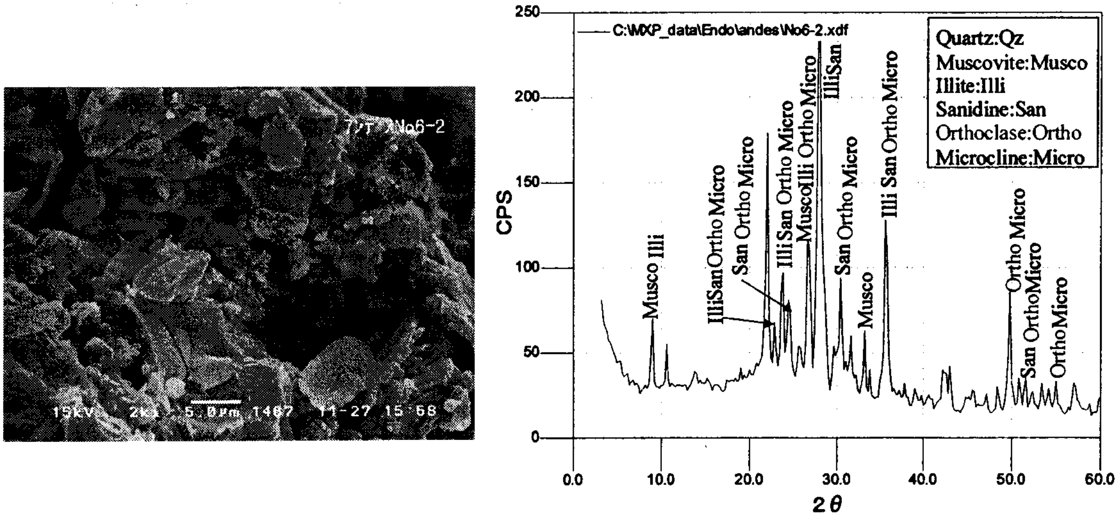

Fig. 2(h). SEM photograph and result by the X-ray diffractometer on pebble sampled at No. 6 site.

Table 1. Mineralogical composition of subsurface including residual soils and intact rock sampled at different sites.

	Quartz	Muscovite	Illite	Sanidine	Orthoclase	Microcline
Intact rock	–	○	○	○	○	○
No. 2-1	–	–	○	○	○	○
No. 2-2	–	○	–	○	○	○
No. 3	○	○	○	○	○	○
No. 5-1	–	○	○	○	○	○
No. 5-2	–	–	○	○	○	○
No. 5 saddle point	–	○	○	○	○	○
No. 6	–	○	○	○	○	○

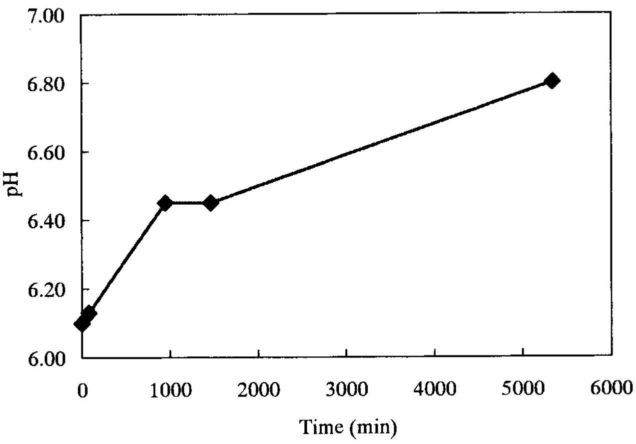

Fig. 3. Relationship between pH value and the time on intact rock sampled from No. 2 site.

general a complicated function of their porosity, permeability, ionic content of pore fluid, and mineral composition. Sakamoto et al. (2000, 2001) carried out resistivity sounding with the Wenner method at eight locations in the Cerro Chascón Science Preserve area. The soil resistivity near the surface was found to be $\leq 1{,}000\ \Omega\mathrm{m}$ at the five locations in the Pampa La Bora area. The values at the three locations in the Llano de Chajnantor area were much higher, exceeding $3{,}500\ \Omega\mathrm{m}$. They concluded that this difference reflects differences in water content in the upper soil layer due to local topography and drainage. The depths of the upper layer of broken rock found at these sites are of order a few meters, and are consistent with depths found from borehole cores obtained.

The resistivity of intact rock sampled from No. 1 boring site was measured in the laboratory to investigate the influence of the water content on the resistivity. Figure 4 shows the layout of the devices for measuring the resistivity. Photo 1 shows the overall view of the measuring device. The device consists of an electric current transmitter, an electric potential measuring device and a sample holder. The holder is made of aluminum and the interface between the holder and the sample is formed with agar that contains potassium chloride solution. In the test, the sample is first cramped with the holder and electric current is poured through the sample from the two electrodes. Then the electric potential difference between the two sides of the electrodes is measured. Based on the measured electric potential difference and the electric current, the resistivity of the sample can be evaluated. The relationship between the electric potential difference and the resistivity can be expressed as:

$$\rho = \frac{V}{I} \cdot \frac{S}{L} \quad (\Omega\mathrm{m}) \tag{1}$$

where, V is electric potential difference, I is electric current, S and L are the area and height of the sample respectively. In order to obtain an accurate value of the area, the diameter and the height of the sample should be measured accurately with a slide calipers.

The transmitted electric current is a direct current that is currently used in normal DC resistance method. The polar of the direct current is changed periodically in order to reduce the influence of the polarization of the

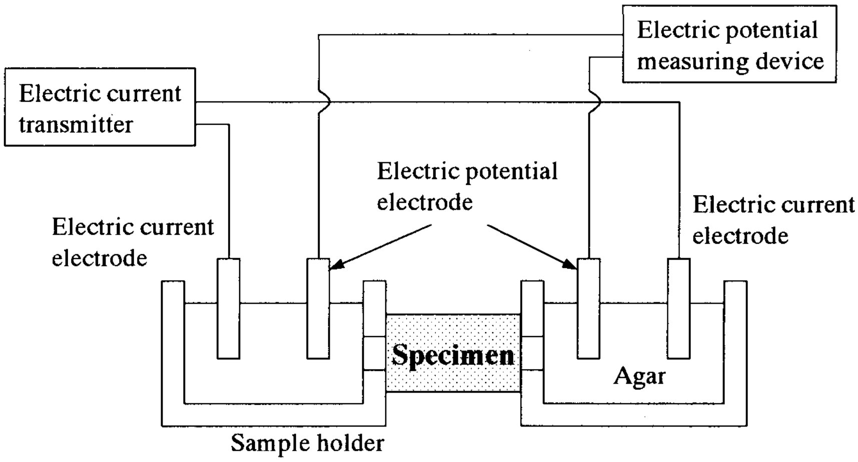

Fig. 4. Layout of the devices for measuring the rock resistivity.

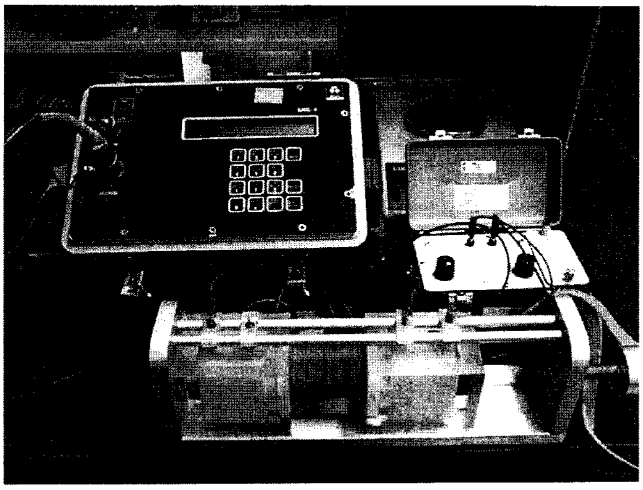

Photo 1. Overall view of the device for measuring the rock resistivity.

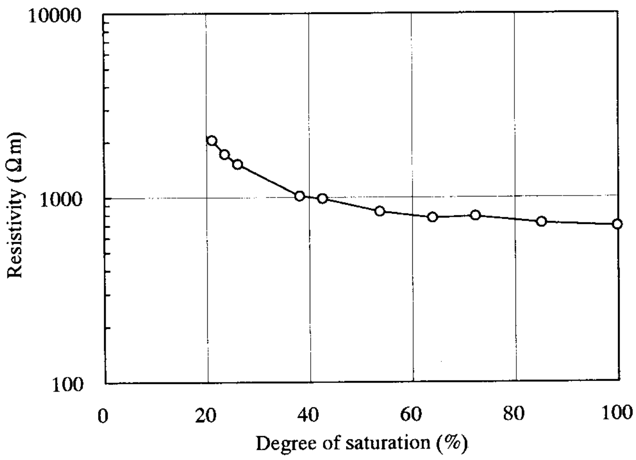

Fig. 5. Variation of the resistivity of the intact rock with respect to degree of saturation.

measuring system. The agar that contains potassium chloride is used in the contact surface between the sample and the holder in order to prevent the deterioration of the surface, which make it possible to obtain a high accurate data.

The resistivity of the sample is measured at different degree of saturation from complete dry to complete saturated. The degree of saturation of the sample is measured after the completion of all measurements, after which the sample is dried with a dry furnace at 110℃.

The degree of saturation is measured in the following sequence:

① Some residual pieces of the sample that formed in the restoration of the sample are firstly saturated and dried to measure the maximum water content.

② Based on ①, the mass and the degree of saturation of the sample are evaluated.

③ Based on ① and ②, the sample is dried naturally to a prescribed saturated degree. The accurate value of the saturation, however, should be calculated under a complete dried condition at last stage.

In saturating a sample, the sample and percolating water (distilled water) are put into a desiccator and evacuated with a vacuous pump. In changing the saturated degree of a sample, instead of using a dry furnace, the sample is dried naturally in air gradually.

The variation of the resistivity of the intact rock with respect to the degree of saturation is summarized in figure 5. The maximum value is consistent with the value obtained at *in situ* measurement by Sakamoto et al. (2000). The resistivity shows a minimum value at a saturated state. It increases according to the decrease in the water content. Based on the results from in situ measurement of resistivity by Sakamoto and present laboratory tests, it is confirmed that the resistivity of the welded tuff is very sensitive to the degree of saturation.

Sakamoto also monitored seasonal and diurnal variation of near-surface soil resistivity. The resistivity shows significant (a factor $\lesssim 3$) seasonal variation with the lowest values during austral summer. The resistivity in summer is $\lesssim 300$ Ωm in the Pampa La Bola area while it is $\lesssim 1,000$ Ωm in the Llano de Chajnantor area. Throughout the year, the resistivity at Pampa La Bola is systematically a factor $\lesssim 3$ lower than at Llano de Chajnantor. Although diurnal variation also exists with lowest values near the sunsets, the peak-to-peak variation is only 3% of the mean value of the day.

Table 2. Results from the ultrasonic wave tests.

Sample number	Sampling depth (m)	Density ρ_t ($g \cdot cm^{-3}$)	Specimen length (cm)	P-wave velocity Vp ($m \cdot s^{-1}$)	S-wave velocity Vs ($m \cdot s^{-1}$)	Poisson's ratio	Young's modulus (MPa)
1	4.90–	2.276	8.060	2,230	1,370	0.198	10,200
2-1	5.45–	2.267	9.950	2,180	1,280	0.236	9,220
2-2	5.45–	2.306	7.930	2,360	1,400	0.231	11,100

3. Geotechnical Study on Foundation

The most important things related to the construction of a foundation of a radio telescope are how to evaluate the modulus of deformation and the strength of the ground. For this reason, uniaxial compression tests on the samples from the six boring sites are conducted. The positions of the boring sites are shown in figure 1. From the tested results, it is known that the strength of the ground is much larger than the pressure of the foundation (about 70 kPa). If considering the environment of the radio telescope where a cyclic load caused by strong wind at highland and a dead weight of the telescope are constantly act on the ground, it is necessary to consider not only a short-term bearing capacity but also a long-term stability of the ground. Besides, it is necessary to understand the characteristics of strength deterioration due to weathering of the welded tuff under environmental changes such as the temperature, the frost and melting of underground water and solar radiation. For these reasons, in addition to the uniaxial compression tests by the reports of NRO and NRAO (2000), a multi-stage uniaxial creep test and slaking test are conducted. E_{50} that stands for the modulus of deformation of a ground at a compression stress equal to 50% of the uniaxial strength of the ground is usually used in the design of a foundation. In constructing a radio telescope, however, the modulus of deformation at small strain level is also very important. Therefore, ultrasonic wave test for measuring the elastic wave speed is also conducted together with the uniaxial compression tests in which a strain gauge is directly pasted on the side face of the sample.

3.1 Rigidity of Rock by Ultrasonic Wave Test

In order to measure the modulus of deformation and Poisson's ratio of the welded tuff at small strain level, ultrasonic wave tests are conducted for measuring the elastic wave speed. The samples used for the tests are from No. 1 boring site at the depth of 4.90 m and No. 2 boring site at the depth of 5.45 m. The diameter of the samples is 57 mm and the length of the samples is 79.3–99.5 mm. Table 2 shows the results from the ultrasonic wave tests.

Based on the speeds of P and S wave of the samples, the Poisson's ratio is evaluated 0.198–0.236, which is almost the same as the value 0.20 obtained from NRO and NRAO (2000) reports. The assumption that Poisson's ratio of intact welded tuff equals to 0.20 is then confirmed to be reasonable.

In NRO and NRAO (2000) reports, the Young's modulus of intact welded tuff estimated by the formula from Hoeck and Brown (1980) based on RMR (Bieniawski, 1988) is about 40,000 MPa. While the Young's modulus estimated from ultrasonic wave tests is about 9,220–11,100 MPa, one fourth of those estimated from NRO and NRAO (2000) reports, with a small dispersion. In spite of the fact that the tested value of Young's modulus is smaller than the estimated value, the modulus is very large compared to the pressure acting on the ground from the telescope. Therefore, the deformation due to the dead load of the telescope will be very small.

3.2 Uniaxial Compressive Strength

In NRO and NRAO (2000) reports, 8 samples from the boring sites were used in uniaxial compression tests. The average value of the uniaxial compressive strength is 21.0 MPa. The value of the uniaxial compressive strength of the sample retrieved from No. 2 boring site is about 40.0 MPa, the maximum value within all the boring sites.

The size of the sample used for the uniaxial compression test is the same as those of ultrasonic wave test, that is, 57 mm in diameter and 99.5 mm in length. The compression test is conducted with strain controlling method, with a strain rate of $0.1\% \cdot min^{-1}$. Figure 6 shows the stress-axial strain relationship, the stress-horizontal strain relationship and the stress-Poisson's ratio relationship. From the figure, it is known that the uniaxial compressive strength is 48.5 MPa, a little larger than the value 40.0 MPa obtained from NRO and NRAO (2000) reports. According to ISO14689 (2001), if uniaxial compressive strength is 5–25 MPa, it is classified as 'weak' and 25–50 MPa is classified as 'medium strong'. According to uniaxial compressive strength obtained from NRO and NRAO (2000) reports, the rock is classified as 'weak rock'. While According to uniaxial compressive strength obtained from present research, it is classified as 'medium strong rock', a rather harder rock even according to the international standard.

In the test, the axial strain is measured with strain gauges and deformation transducer installed outside the sample. Because of the influence of bedding error at the two head faces, the strain measured by outside deformation transducer is larger than those measured from strain gauges. This influence can also be observed in failure strain. The failure strain from outside deformation transducer is about 0.463% while that from the strain gauges is only about 0.365%. The failure strain of intact welded tuff is found to be very small and less than 0.5%.

The moduli of deformation E_{50} measured by outside deformation transducer and strain gauge are 12,400 MPa and 15,400 MPa respectively. These values are little larger than those evaluated from ultrasonic wave tests but much

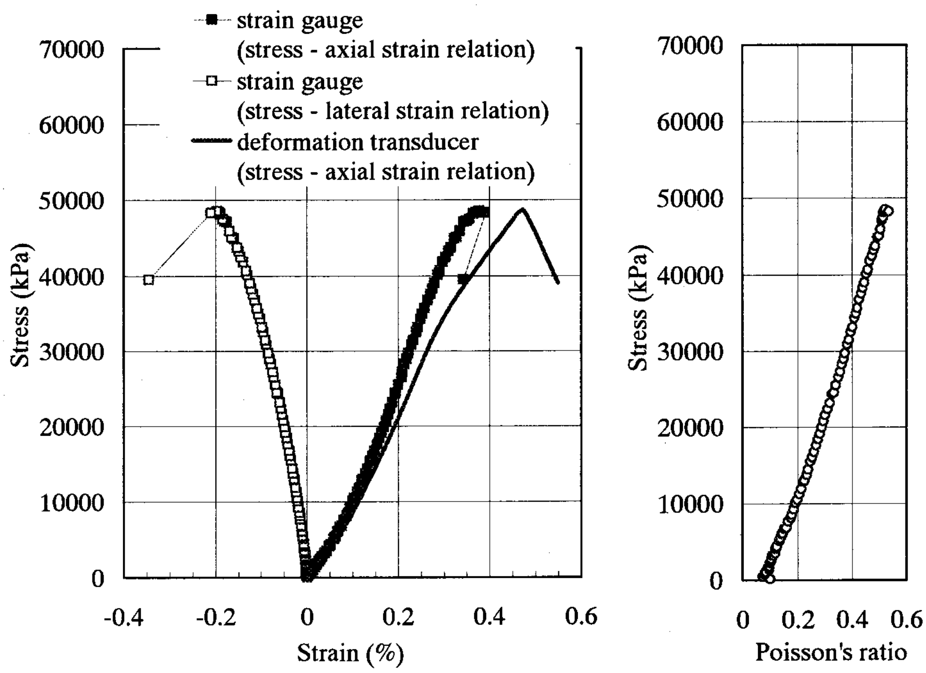

Fig. 6. Stress-axial strain relationship, the stress-horizontal strain relationship and the stress-Poisson's ratio relationship.

Table 3. Rock stability in water (ISO/DIS 14689, 2001).

Term	Description (after 24 hrs in water)	Grade
Stable	No changes.	1
Fairly stable	A few fissures are formed, or specimen surface crumbles a bit.	2
	Many fissures are formed and broken into small lumps, or specimen surface considerably crumbles.	3
Unstable	Specimen disintegrates, or nearly whole the specimen surface crumbles.	4
	Whole the specimen becomes muddy, or disintegrates into sand.	5

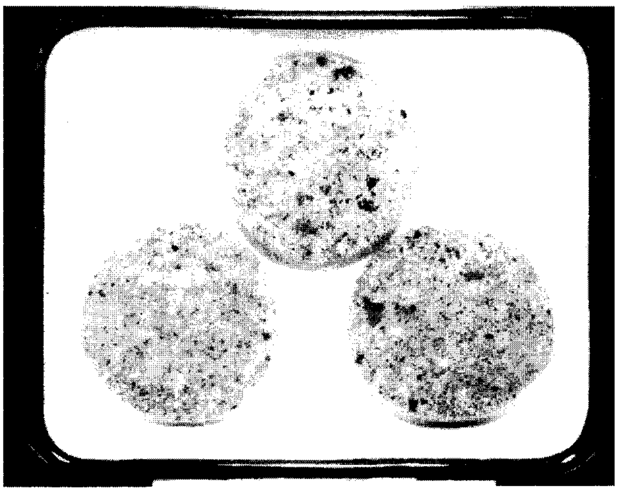

Photo 2. Three samples in water for 24 hours.

smaller than those estimated in NRO and NRAO (2000) reports. The Poisson's ratio obtained by the ratio of the horizontal strain to axial strain is also shown in the figure and its value at E_{50} is about 0.3, being a little larger than those from ultrasonic wave tests. This means that at the stage when axial stress reaches the 50% of the uniaxial compressive strength, plastic strain has already occurred. In very small stress level, Poisson's ratio will be about 0.1 while at the failure state, it will be near 0.5.

3.3 Potential for Deterioration of Rock

During the working period of the radio telescope, it is necessary to understand the characteristics of strength deterioration due to weathering of the welded tuff under environmental changes such as the temperature, the frost and melting of underground water and solar radiation. For this reason, a simplified slaking test is conducted. The sample used in the test is from Boring No.1 site. Three samples with a thickness of 20 mm are prepared and immersed in a palette for 24 hours, as shown in Photo 2.

According to ISO14689 (2001), the state change of the sample after 24 hours immersed in water is classified to 5 grades whose deteriorated behavior are described in Table 3. In present tests, however, no change can be observed at all, which means that the sample is classified as Grade 1. Therefore, it is known that the welded tuff is hard to deteriorate.

3.4 Long Term Strength of Rock

During the working period of the radio telescope, if considering the environment of the radio telescope where a cyclic load caused by strong wind at highland and a dead weight of the telescope are constantly act on the ground, it is necessary to consider not only the short-term bearing capacity but also the long-term stability of the ground. For this reason, in order to make full use of the available samples, a multi-stage uniaxial creep test is conducted. The sample used in the test is from No. 2 site. The size of the sample, according to the capacity of the test machine, is trimmed to 34.7×79.3 mm in diameter and length.

The test is conducted in following sequence:

① A uniaxial compression test is firstly conducted on the sample neighboring to the sample for the creep test to obtain the uniaxial compressive strength (48.5 MPa). This value is taken as the standard strength.

② Uniaxial creep test under 70% of the standard strength (33.95 MPa) is conducted for 2,882.8 min.

③ Uniaxial creep test under 80% of the standard strength (38.80 MPa) is conducted for 4,209.9 min.

④ Uniaxial creep test under 90% of the standard strength (43.65 MPa) is conducted for 4,321.9 min.

⑤ Uniaxial creep test under 95% of the standard strength (46.08 MPa) is conducted for 5,943.0 min.

⑥ Uniaxial creep test under 98% of the standard strength (47.53 MPa) is conducted for 11,860.3 min. up to final failure.

Figure 7 shows the strain rate-time relationship. The axial strain and lateral strain are measured by the strain gauges directly pasted at the sample at different loading stages. It is found from the figures that the rock is very strong and creep failure happened at the stress level very near to the uniaxial compressive strength. The omen of the creep failure is the outstanding development of the lateral strain of the sample. It can be concluded that there is no problem in the long-term stability of the welded tuff.

4. Conclusions

The following conclusions can be given according to the research conducted in this paper:

1. Alkali-aggregate reaction might take places because Sanidine that shows alkali is involved in the rock. Therefore, more detail discussion on the prevention of the alkali-aggregate reaction in the concrete foundation should be done.
2. The resistivity of the welded tuff is very sensitive to the degree of saturation. The larger the water content is, the smaller the resistivity will be.
3. The Young's modulus is very large; therefore, the deformation due to the dead load of the telescope will be very small.
4. The failure strain of intact welded tuff is very small and less than 0.5%.
5. According to the uniaxial compressive strength obtained from present research, the welded tuff is classified as 'medium strong rock', a rather

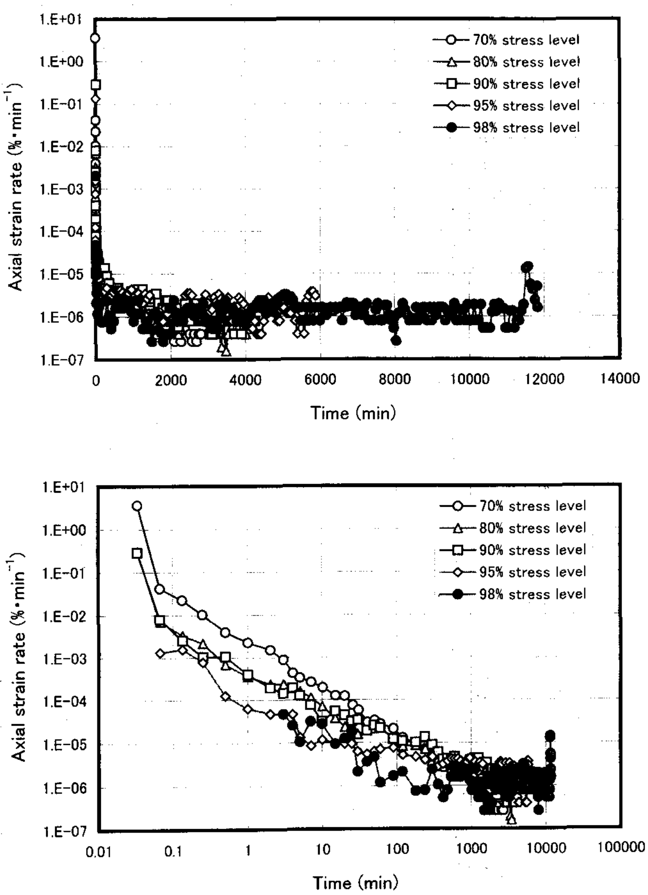

Fig. 7(a). Relationship between axial strain rate and time.

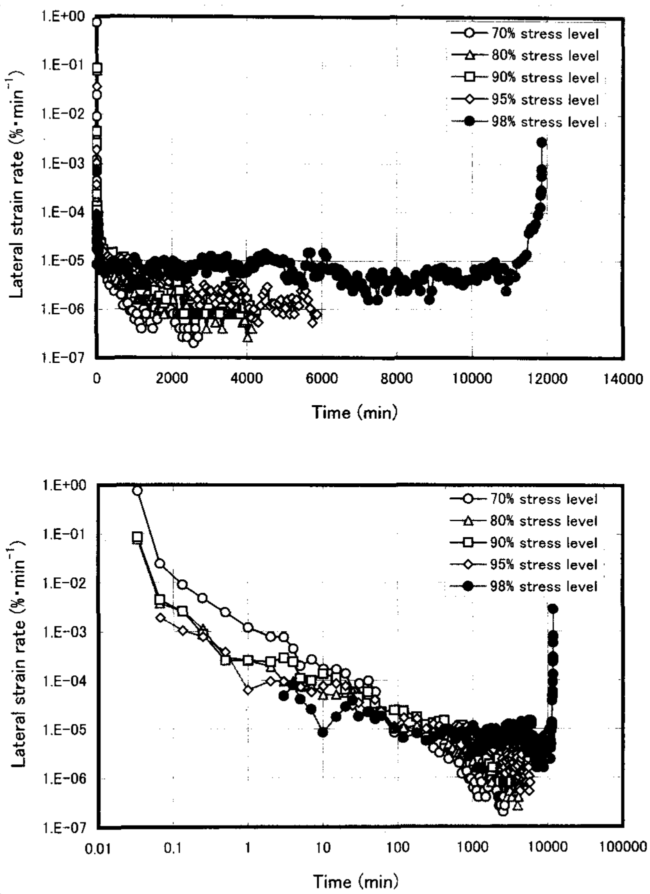

Fig. 7(b). Relationship between lateral strain rate and time.

harder rock even according to the international standard.

6. The welded tuff in the construction site is hard to deteriorate.
7. There is no problem in the long-term stability of the welded tuff.

REFERENCES

Bieniawski, Z. T. 1988, The Rock Mass Rating (RMR) System (Geomechanics classification) in engineering practice, *ASTM STP*, 984.

Hoeck, E., and Brown, E. T. 1980, Underground excavations in rock, The Institution of Mining and Metallurgy, London.

ISO 2001, Identification of soil and rock, Revised manuscript of ISO/DIS 14689.

NRO-NRAO 2000, Geotechnical study, Chajnantor Site, II Resion, *LMSA Memo*, 2000–2004.

Sakamoto, S., Ezawa, H., Takahashi, T., and Yamaguchi, N. 2000, Vertical profiles of soil resistivity at Pampa La Bola and Llano de Dhajnantor Locations, *ALMA Memo*, No. 326.

Sakamoto, S., and Sekiguchi, T. 2001, Spatial distribution of near-surface soil resistivity in the Cerro Chascón Science Preserve, *ALMA Memo*, No. 346.